THE JOURNAL OF PHYSICAL CHEMISTRY C

pubs.acs.org/JPCC Article

Effect of Molecule−Substrate Interactions on the Adsorption of *meso*-Dibenzoporphycene Tautomers Studied by Scanning Probe Microscopy and First-Principles Calculations

Tomoko K. Shimizu, Carlos Romero-Muñiz, Oleksandr Stetsovych, Jaime Carracedo-Cosme, Michael Ellner, Pablo Pou, Koji Oohora, Takashi Hayashi, Ruben Perez,* and Oscar Custance*

Cite This: *J. Phys. Chem. C* 2020, 124, 26759−26768 Read Online

ACCESS | Metrics & More | Article Recommendations | Supporting Information

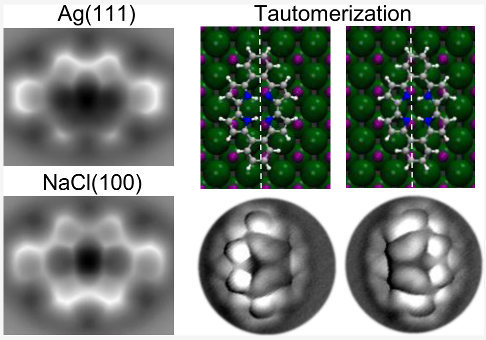

ABSTRACT: *meso*-Dibenzoporphycene molecules adsorbed on the Ag(111) surface and on 2-monolayer-thick NaCl films were studied using submolecular resolution atomic force microscopy (AFM), scanning tunneling microscopy (STM), and first-principles calculations to clarify their stability and tautomerization behavior. We have found that the bonding of the molecules with the surface is determined by the interplay of different contributions, including the interaction of the π-aromatic orbitals of the benzene rings and the metal-coordination bond of the lone-pair electrons of the imine nitrogen atoms with the metal atoms (Ag, Na) on each substrate. The strength of the latter ultimately governs the molecular adsorption configuration and determines the nature and energy barriers for tautomerization. On Ag(111), the interaction of the imine nitrogen atoms with the Ag atoms deforms the macrocycle of porphycene, leading to a distinct AFM contrast that allows a clear identification of the molecule in its cis tautomeric form. In contrast, on NaCl films, the weaker interaction with the Na atoms leads to a flatter geometry and very similar adsorption configurations for the cis- and trans-forms, which cannot be distinguished in AFM experiments. Although weak, the dominant role of this local N−Na interaction, compared to the essentially nondirectional dispersive interactions, results in a new type of tautomerization process. In this case, the transfer of hydrogen atoms within the porphycene cavity is accompanied by a significant displacement of the whole molecule to a new site to reach a new minimum energy adsorption configuration. Our theoretical calculations indicate that this lateral translation, rather than the intramolecular H transfer, dominates the activation energy on NaCl. This novel tautomerization behavior, which we have identified on a rather inert ionic surface, might also be present on other weakly interacting substrates.

■ INTRODUCTION

Tautomerization reactions, where hydrogen (H) atoms are transferred within the molecule have been proposed as a potential molecular switch. Porphyrin and phthalocyanine derivatives are prototypical molecular systems to study tautomerization reactions. H migration within the central cavity of porphyrin and phthalocyanine molecules can be monitored at a single molecular level using scanning tunneling microscopy (STM).[1−5] The tautomerization behavior of porphycene (Pc)—a constitutional isomer of porphyrin—differs from the case of porphyrin and phthalocyanine due to a symmetry break provided by the rectangular shape of its central cavity.[6] The H-bonds between the hydrogen of amine NH and imine N on the other side in the cavity of Pc are stronger than those of porphyrin because of the shorter distances between N atoms, which reduce the activation barrier to accelerate the H transfer reaction.[7,8] Several STM studies have revealed the structure, stability of tautomers, and stimuli-induced tautomerization reactions of Pc adsorbed on noble metal surfaces.[8−16] Although, the trans-form is, in general, more stable than the cis-form in the gas phase, the potential energy landscape for the tautomerization reaction can be altered by the presence of the substrate, favoring the cis-form for some adsorption configurations. For example, the cis tautomeric form of Pc was found to be more stable than the trans-form on the Cu(110) and Ag(110) surfaces due to the strong binding of nitrogen (N) lone-pair electrons in the Pc cavity to metallic atoms, leading to a nonplanar configuration with the deformation of the macrocycle.[8,9,16] On the Cu(111) and Ag(111) surfaces, the trans-form is thermodynamically stable, but trans to trans tautomerization is not observed,[15,17] which is a different behavior from the porphyrin and

Received: August 24, 2020
Revised: November 3, 2020
Published: December 1, 2020

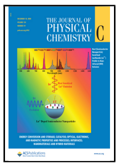

https://dx.doi.org/10.1021/acs.jpcc.0c07726
J. Phys. Chem. C 2020, 124, 26759−26768

phthalocyanine families.[1−5] On the Au(111) surface, a weaker Pc—Au interaction leads to either a rapid tautomerization rate or to a very similar character of the molecular orbitals of both forms, which hampers the discrimination between the cis and trans tautomers.[15] Based on these experimental results, the strength of the molecule—substrate interaction is expected to govern the energetics of tautomerization. Recent theoretical analysis using dispersion-inclusive density functional theory (DFT) calculations also demonstrated that as the adsorption energy of Pc on metals increased from Ag to Cu, Pd, and Pt, the barrier for the tautomerization also increased in this order.[18]

Slight differences in the molecular structure may also generate different adsorption configurations, and thus it is of great interest to study derivatives of a mother molecule. Various Pc derivatives have been reported,[19,20] but among them *meso*-dibenzoporphycene (mDBPc) produced by fusing two benzene moieties at the ethylene-bridged positions of Pc is of particular interest.[21] The main characteristics of mDBPc is a further delocalization of the π-electrons than in the case of Pc, resulting in light absorption in the infrared region.[20,21] The cis-form of this molecule becomes the ground state even in the gas phase, in contrast to other porphyrin and phthalocyanine derivatives that exhibit the trans-form as the most stable tautomer.[19,22] The trans and cis-forms of the mDBPc molecule are shown in Figure 1a,b (see also Figure S1). The central Pc cavity contains four N atoms (each in a pyrrole ring), two of them saturated with H atoms (amine N's) and the other two unsaturated (imine N's). When mDBPc molecules are adsorbed on a solid surface, the two additional benzene moieties should provide a stronger attractive interaction with the substrate than a normal Pc, via a π-orbital overlap or a van der Waals (VDW) interaction. Depending on the balance between the bonding strength at the imine N's and the dispersion force acting at the benzene moieties, the adsorption configuration and the resulting tautomerization behavior may significantly differ from those of normal Pc.

Here, we report a study on the adsorption behavior of mDBPc molecules on the Ag(111) surface and on a 2-monolayer (ML)-thick sodium chloride (NaCl) film/Ag(111) using submolecular resolution atomic force microscopy (AFM) and STM. The presence of a 2-ML-thick NaCl film between the molecule and the metal surface gives rise to an even weaker molecule-surface interaction than in the case of a Au(111) substrate, and reduces the orbital hybridization with metal electronic states as well as the charge transfer between the molecule and metal. This decoupling from the metallic surface is evidenced by the similarity of the spatial distribution of the frontier orbitals of molecules adsorbed on the NaCl film and those in the gas phase.[2,23] We found that while the binding mechanism of the cis tautomeric form of mDBPc on Ag(111) is quite similar to those of Pc on noble metal surfaces, on the NaCl film it differs significantly: we observed two distinct appearances of mDBPc on NaCl, which are related to their adsorption orientation with respect to the NaCl lattice rather than to the tautomeric forms. Our first-principles calculations reveal that, due to the difference in the interaction strength, the activation barriers for the tautomerization on NaCl are smaller than those on the metallic substrates and closer to those found in the gas phase. The difference from the free molecule case can be traced back to the distinct nature of the molecule—substrate interaction on NaCl that tends to accommodate the lone pair of imine N atoms on top of Na atoms. Upon a H transfer, this interaction, although weak, is strong enough to induce a lateral translation of the entire molecule. This translation yields the dominant contribution to the tautomerization barrier rather than the intramolecular H transfer.

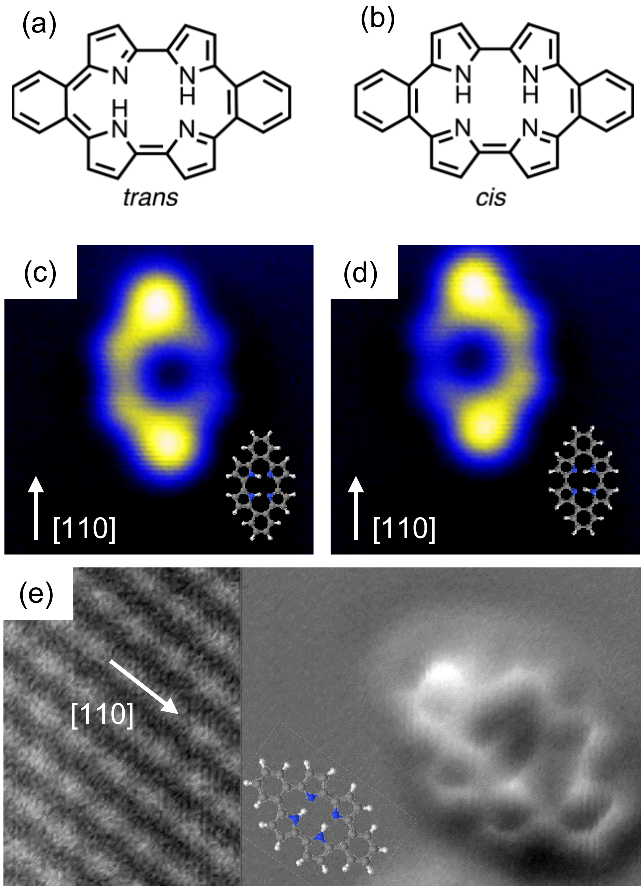

Figure 1. (a and b) Chemical structures of the trans (a) and cis (b)-forms of the mDBPc molecule. (c−e) STM and atomic force microscopy (AFM) images of the mDBPc molecule adsorbed on the Ag(111) surface. (c and d) Constant-height tunneling current (I_t) images before (c) and after (d) a flip over the long molecular axis induced by a voltage pulse. The flip was accompanied by a lateral translation along the [110] direction of the Ag(111) surface. (e) Constant-height frequency shift (Δf) image of an mDBPc molecule on Ag(111). The left part of the image was recorded scanning closer to the surface to atomically resolve the Ag lattice. The right part of the image was obtained with the probe lifted from the surface by 400 pm to image the mDBPc with submolecular resolution. The insets in the images show the corresponding molecular model. The color code for the ball-and-stick model is blue for nitrogen atoms, gray for carbon atoms, and white for hydrogen atoms. The scanned areas were (2.5 nm × 2.5 nm) for (c) and (d) and (4 nm × 2 nm) for (e). The sample bias values were V_s = 100 mV for (c) and (d) and V_s = 1 mV and 5 mV for the left (Ag area) and the right (mDBPc area), respectively, in (e). The I_t color scale was from 2.2 (dark blue) to 10.7 pA (yellow-white). The Δf gray scale in the Ag lattice region was from −0.34 (black) to −0.14 Hz (white) and in the mDBPc region from −0.38 (black) to +0.50 Hz (white).

■ METHODS

Experiment. A home-built ultrahigh vacuum (UHV) cryogenic scanning probe microscope (SPM) and a commercial SPM controller (Nanonis SPM Control Systems, SPECS, Germany) were used for the experiments. We used the KolibriSensor for the simultaneous detection of the tunneling current (I_t) and probe-surface interaction forces. The bias voltage (V_s) was applied to the sample. An AFM was operated in frequency modulation detection mode,[24] keeping the oscillation amplitude constant. Measurements were performed at 4.8 K. Prior to measurements, the probe of the KolibriSensor was sharpened to a typical apex radius of ~15 nm using an *ex situ* focused ion beam and further conditioned for atomic resolution imaging *in situ* on the clean area of the Ag(111) surface. The probe was functionalized with a carbon monoxide (CO) molecule using similar techniques as reported elsewhere[25,26] and used for submolecular resolution imaging.

A single crystal Ag(111) was cleaned by repeated cycles of Ar^+ ion sputtering at 1 kV for 10 min and annealing at 770 K for 10 min in UHV. NaCl was evaporated *in situ* on the clean Ag(111) surface at submonolayer coverage at room temperature, resulting in the formation of 2−3-monolayer (ML)-thick NaCl islands. The sample was then transferred to the microscope stage and cooled down to 4.8 K. The mDBPc molecules were synthesized according to the recipe reported elsewhere.[21] Their powder was further purified by degassing in a homemade Knudsen cell installed in a UHV chamber. mDBPc was evaporated by heating the cell to 570−600 K while keeping the Ag(111) crystal below 30 K temperature at the microscope stage. The deposition at such a low temperature suppressed molecular diffusion, so some of the mDBPc molecules could be found on the NaCl islands. CO molecules were deposited on the surface while keeping the Ag(111) crystal below 16 K temperature by back filling the microscope chamber with CO gas and opening the shutters of the radiation shield at the cryostat. When CO molecules were found near the mDBPc molecules, we used lateral manipulation techniques[27] to move the CO molecules away to obtain isolated single mDBPc molecules. We examined and performed experiments on mDBPc molecules adsorbed on the Ag(111) surface as well as on the 2-ML-thick NaCl islands.

Theory. Our simulations are based on density functional theory calculations following the implementation provided in the VASP code.[28] An energy cutoff for the plane-wave basis set of 400 eV was used in combination with pseudopotentials constructed after the PAW method.[28,29] The Perdew−Burke−Ernzerhof functional[30] was chosen to reproduce the electronic exchange and correlation, supplemented by the D3 semi-empirical correction[31] to account for the dispersion interactions. The adsorption of the mDBPc molecules was studied on both Ag(111) and NaCl(100) to compare with experimental results. The Climbing Image Nudged Elastic Band (CI-NEB) method[32] has been used to find the minimum energy paths for the on-surface tautomerization processes. The zero-point energy (ZPE) correction to the transition state energy has been taken into account. We have considered the vibrational energies of the normal modes associated with the amine groups in the mDBPc molecule, following the procedure detailed in the previous work.[12,16] From the input from the DFT calculations described above, we used our recently developed method to simulate the AFM images.[33] This approach merges different ideas presented in previous studies to describe the different interactions and retains DFT accuracy with just two fitting parameters. Moreover, our model describes both the electrostatic (ES) and short-range (SR) interactions in terms of two physical observables: the total charge densities of the sample and the functionalized probe, which are obtained from independent ab initio calculations. A detailed description of this method and its performance can be found in our previous studies.[33−35] Further details of the computational methods used in this work can be found in the Supporting Information.

RESULTS AND DISCUSSION

mDBPc molecules stably adsorb on the Ag(111) surface. In STM images, they appear as elongated ovals, asymmetric with respect to the long axis of the molecule, with one side brighter than the other, as it is shown in Figures 1c and S2a. The molecule central part appears as a dark hollow. Two bright areas at the ends of the long molecular axis are attributed to the benzene moieties fused to the *meso* positions of the central Pc framework. A high-resolution AFM image of the same molecule further reveals details about its structure (Figure S2c). The two pyrrole rings located at the bright side of the STM image are clearly visible in the AFM signal, whereas the other two rings at the opposite side present a faint AFM contrast. To determine the adsorption site of the mDBPc molecule, we measured a constant-height AFM image acquired at two different probe-surface separations exhibiting both atomic resolution on the Ag(111) surface and molecular contrast over the mDBPc (Figure 1e). The superposition of an atomic lattice over the Ag(111) region allowed us to find that the long molecular axis is parallel to the [110] direction, and that the two N atoms at the faint pyrrole rings seem to be located close to two adjacent Ag atoms (Figure S3). This strategy allows us to infer the position of these N atoms, which cannot be resolved in the AFM images, with respect to the substrate. This adsorption site is quite similar to the one exhibited by the cis-form of a normal Pc adsorbed on the Cu(110), Cu(111), and Ag(111) surfaces.[8−10,15] The interatomic distances along the <110> directions on these three surfaces are 255 pm for Cu(110) and Cu(111), and 289 pm for Ag(111). On these substrates, the lone-pair electrons at the two imine N's interact with the adjacent metal atoms underneath, resulting in a slight difference in height between the imine and amine sides, and leading to the asymmetric appearance of the cis-form of Pc.[8,15] The same interpretation can be applied to the adsorption of mDBPc on the Ag(111) surface: the asymmetric appearance can be attributed to the cis-form, where the imine side of the central Pc cavity is located closer to the substrate than the amine side. Note that the distance between two N atoms in the mDBPc crystal is 294 pm, and calculated values in the gas phase are 290−294 pm,[21] which match well with the interatomic distances of Ag on the substrate.

We can induce the movement of the mDBPc molecules on the Ag(111) surface by applying bias voltage pulses. The molecule hops in the direction of the long molecular axis when a pulse is applied on one of the fused benzene rings. It is also possible to induce the flip of the molecular appearance along the long molecular axis, i.e., the bright and dim sides of the STM image exchange by applying a voltage pulse at the brighter side of the central Pc cavity. This event can be attributed to a cis- to cis- tautomerization with the transfer of two H atoms in the Pc cavity from one side to the other. The STM images in Figures 1d and S2b show the same mDBPc molecule as the one in Figures 1c and S2a, but after inducing this cis- to cis- tautomerization. The corresponding AFM images are also displayed in Figure S2d. The reaction is always accompanied with a small lateral displacement along the long molecular axis (<110> direction), with the new adsorption site equivalent to the previous one. These induced flips are quite

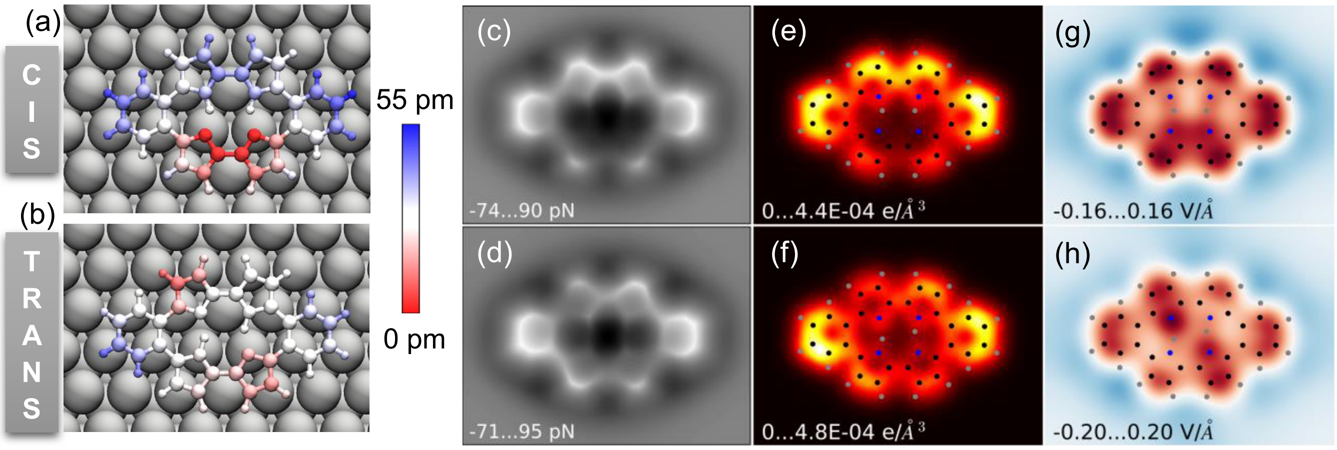

Figure 2. (a and b) Most stable structures for the cis and trans-forms of the mDBPc molecule adsorbed on the Ag(111) surface obtained from first-principles simulations. The color scale of the molecule represents the height of the atoms upon adsorption on the surface. 0 pm is set to the position of the atom closest to the substrate, and the white color in the color bar is associated with the surface−molecule distance at the mean plane (defined as the average of the z coordinates of all of the atoms in the molecule), The mean planes for (a) and (b) are 297 pm and 305 pm, respectively. (c and d) Calculated constant-height force maps for the cis (c) and trans (d) forms of the mDBPc molecule on Ag(111). The probe height is 3.1 Å from the average molecular plane. The black-to-white color codes for the force range are from −74 to 90 pN for the cis-form and −71−95 pN for the trans-form. (e and f) Calculated charge density maps, at 3 Å from the average molecular plane, of the cis and trans-forms of mDBPc adsorbed on Ag(111), respectively. The highest charge density is expressed in yellow and the lowest charge density in black. (g and h) Simulated vertical component of the electric field, at 3 Å from the molecular plane, created by the cis and trans-forms of mDBPc adsorbed on Ag(111), respectively. The highest positive value (electron attraction) is expressed in blue and the lowest (electron repulsion) in red. In (e, f, g, h), the small dots represent the positions of atoms within the molecule: black for C, blue for N, and gray for H.

similar to those of Pc adsorbed on the Cu(110) surface,[8] but different from Pc on the Ag(111) surfaces; in the latter, both the cis and trans-forms are present and the energy required to induce a cis- to cis- tautomerization is very low.[15] This difference is considered to arise from a stronger adsorption energy for the mDBPc than for the Pc due to the additional interaction of the two benzene moieties with the surface.

The adsorption energy for the mDBPc on Ag(111) is 3.70 eV, calculated with DFT first-principles calculations as implemented in the VASP package,[28] using plane waves with an energy cutoff of 400 eV, PBE + D3[30,31] as the exchange correlation functional and PAW pseudopotentials[29,36] (see Methods for more details). This value is not far from but larger than the one of Pc on Ag(111).[15] The theoretically obtained adsorption configuration with the height variations of atoms of the cis-mDBPc upon adsorption is shown in Figure 2a. In the cis-form, the two imine N's are located closer to the Ag substrate than the amine N's by ∼36 pm, in good agreement with the experimental observations. The adsorption configuration of the trans-mDBPc is shown in Figure 2b. Although the adsorption site of the trans-form is almost identical to that of the cis-form, the trans-form is energetically less favorable by 40 meV, leading to a flatter geometry, as it is shown by the color variation. Simulated force maps of both cis- and trans-forms (Figure 2c,d, respectively) also support the assignment of the experimental images to the cis-form. In the cis-form, the amine side of the Pc cavity appears brighter than the imine side, whereas that of the trans-form shows a slightly more symmetric shape. Because the dominant contribution to submolecular resolution AFM imaging is the short-range force exerted at the probe apex, the main features in the AFM images resemble the charge density maps of the molecule (Figure 2e,f) with minor contributions from the electrostatic potential, which are reflected in the electric field maps (Figure 2g,h).[33,35,37,38]

Notice that the charge density at the height range explored by the CO-probe has significant contributions not only from the topmost atoms in the adsorption configuration but also from those atoms contributing to molecular orbitals that decay slowly into the vacuum. The interplay of these two features ultimately controls the contrast observed in the AFM image, as discussed below.

In contrast to the adsorption on the Ag(111) surface, two types of appearances of the mDBPc molecules are observed on the 2-ML-thick NaCl films. We found that these two different appearances are not related to the two tautomeric forms but to distinct orientations of the molecule on the surface. Figure 3a is an AFM image of the mDBPc molecule adsorbed with its long axis parallel to the [110] direction of the NaCl lattice, as highlighted in Figure S4a, by the superposition of a lattice grid over the NaCl atomic positions, (hereafter we use the notation "configuration A" to describe this adsorption configuration). The other orientation ("configuration B") is rotated by 45°: the long molecular axis is aligned with the [100] direction of the NaCl lattice, as it is shown in Figures 3b and S4b. While configuration A appears asymmetric with respect to the long molecular axis, configuration B displays a symmetric shape with four pentagonal pyrrole rings visible in the Pc frame—which could imply that the four N atoms in the Pc cavity are equivalent in terms of height and chemical state. The adsorption site of the molecule in configuration B is such that the center of the molecule is located on top of a Na atom. Reversible transformations between asymmetric configuration A and symmetric configuration B are achieved by applying voltage pulses that simultaneously induce the rotation and lateral displacement of the molecule.

One might expect that configuration A on the NaCl surface would resemble the adsorption configuration on the Ag(111) surface. The calculated adsorption energy on NaCl is, however, much smaller than that on Ag(111) (2.14 eV on NaCl; 3.70 eV on Ag(111)). The adsorption site is so as to minimize the Pauli

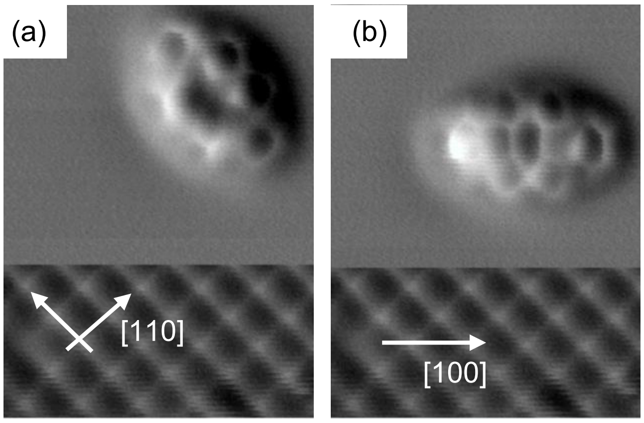

Figure 3. (a and b) Constant-height Δf images of an mDBPc molecule adsorbed on a bilayer thick NaCl island before (a) and after (b) a displacement induced by a voltage pulse. The lower part of the image was scanned at a closer distance toward the surface to reveal the atomic lattice of NaCl. The probe was then slightly lifted up from the surface to resolve the mDBPc with submolecular resolution. The protrusions in the NaCl lattice corresponds to the Cl ions. The two orientations of the mDBPc molecule are referred to in the text as configuration A for (a) and configuration B for (b). The scanned area was (3 nm × 4 nm). The sample bias values were V_s = 150 mV for (a) and V_s = 100 mV for (b). The Δf gray scale in both images was from −0.3 (black) to +0.5 Hz (white).

repulsion between the π-orbitals of the two benzene moieties and the Cl ions underneath as well as to maximize the attraction with the imine groups. The adsorption energy of the trans-form on the same adsorption site is slightly smaller than that of the cis-form: 2.11 eV. Notice that, in this case, only one nonsaturated N atom of imine interacts with a Na atom of the substrate.

The strength of the molecule−substrate interaction influences the adsorption configuration and therefore the force sensed by the probe. Figures S5−S7 illustrate the dependence of the frequency shift (Δf) signal with the probe-sample separation measured over an mDBPc molecule adsorbed on Ag(111), as well as over molecules in configuration A and configuration B on a 2-ML-thick NaCl island, respectively. As the probe approaches toward the molecule on the Ag(111) surface, it first senses the benzene moieties, and then the pyrrole rings of the amine side followed by the imine side. In contrast, for the molecule in configuration A on the NaCl surface, the probe feels the outer part of the faint pyrrole rings (imine side) first, and later those of the amine side and benzene moieties. The imine side appears the brightest for the NaCl cases, at the distance where submolecular contrast starts to appear. This is opposite to the case of Ag(111), where the amine side is always brighter than the imine one. Configuration B on NaCl also differs from the other two cases. The probe starts to feel a repulsive interaction with one of the benzene moieties even at relatively far separations. The interaction at the four pyrrole rings is very similar, though there are some small variations probably due to slight asymmetry at the apex of the probe. The force-induced tautomerization reactions reported for the case of porphycene on Cu(110)[15] were not observed during the spectroscopy measurements we have done on the mDBPc molecules with the AFM. This is probably because we were using a CO-functionalized probe in these experiments, which renders the apex chemically inert.

The calculated constant-height force maps (Figure 4e,f) obtained from the optimized adsorption geometries for the cis and trans-forms (Figure 4a,b, respectively) of the mDBPc molecule in configuration A on NaCl(001) confirm that it is quite challenging to distinguish between the two tautomeric forms using AFM. The simulated images of both tautomers resemble the experimental ones: the outer part of the two pyrrole rings at the imine side is the brightest; the two pyrrole rings of the amine side are clearly visible; and, the two benzene moieties also show a high contrast, more pronounced at the amine side. Furthermore, the variation with respect to the probe-sample separation also shows a good agreement with the experiments, see for example the cis-form in Figure S8. The calculated charge density maps of cis- and trans-forms (Figure 4i,j), which are closely related to the short-range force detected in the experiments, do not show significant differences. The maps of the vertical component of the electric field (Figure 4m,n) reflect the H-atom positions and thus the two tautomeric forms appear different. The contribution of this electrostatic potential to the total force acting at the probe is, however, practically undetectable. The spatial distribution of the total force (TOT) as well as the short-range (SR), electrostatic (ES), and van der Waals (VDW) force components were also simulated, as shown in Figure S9; in all of these images, the positions of the H-atoms are not clearly discerned. Taking into account the full relaxation of the CO molecule at the probe apex (Figure 4e,f, and TOT Rel in Figure S9b), the calculated force image shows a smoothening of the molecular features and a sharpening of the lines between the atomic positions, but it does not improve the detection of the H atoms within the Pc cavity.

The distinction between the two tautomers is also challenging when the mDBPc molecule is in configuration B. As it is shown in Figure 4g,h, the calculated force maps for the cis- and trans-forms obtained for the optimized structures shown in Figure 4c.d are again quite similar. Upon inspecting the different contributions to the calculated force maps, the total (TOT) and short-range force (SR) images show the amine N sites slightly brighter than the imine N sites, but this distinction blurs out when the relaxation of the CO molecule at the probe apex is taken into account. As discussed above, the AFM image contrast is not only controlled by the topmost atoms of the molecule in the adsorbed configuration, but it has a significant contribution from the relatively slow decay of filled orbitals close to the Fermi level.[29] There are no remarkable differences between the cis and the corresponding trans conformers. This finding supports the experimental images showing 4-fold symmetry around the central Pc cavity (Figures 3b and S7).

Similar to the Ag(111) case, it is also possible to induce a flipping in the appearance of the mDBPc molecule in configuration A on the NaCl surface. The flip occurs by setting a bias voltage of a magnitude above 100 meV. In Figure 5, a comparison between experimental AFM images of an mDBPc molecule obtained by scanning at the constant-height with sample bias values of +10 mV (Figure 5a,b), −300 mV (Figure 5c,d), and +500 mV (Figure 5g,h) are shown. The asymmetric shape of the molecule is preserved at a lower bias voltage (Figure 5a,b). On the contrary, the molecular shape becomes symmetric, displaying four equivalent pyrrole rings, when the images are acquired at higher bias voltages (Figure 5c,d,g,h). This delusive symmetry is due to the constant flipping of molecule's appearance over the long molecular axis

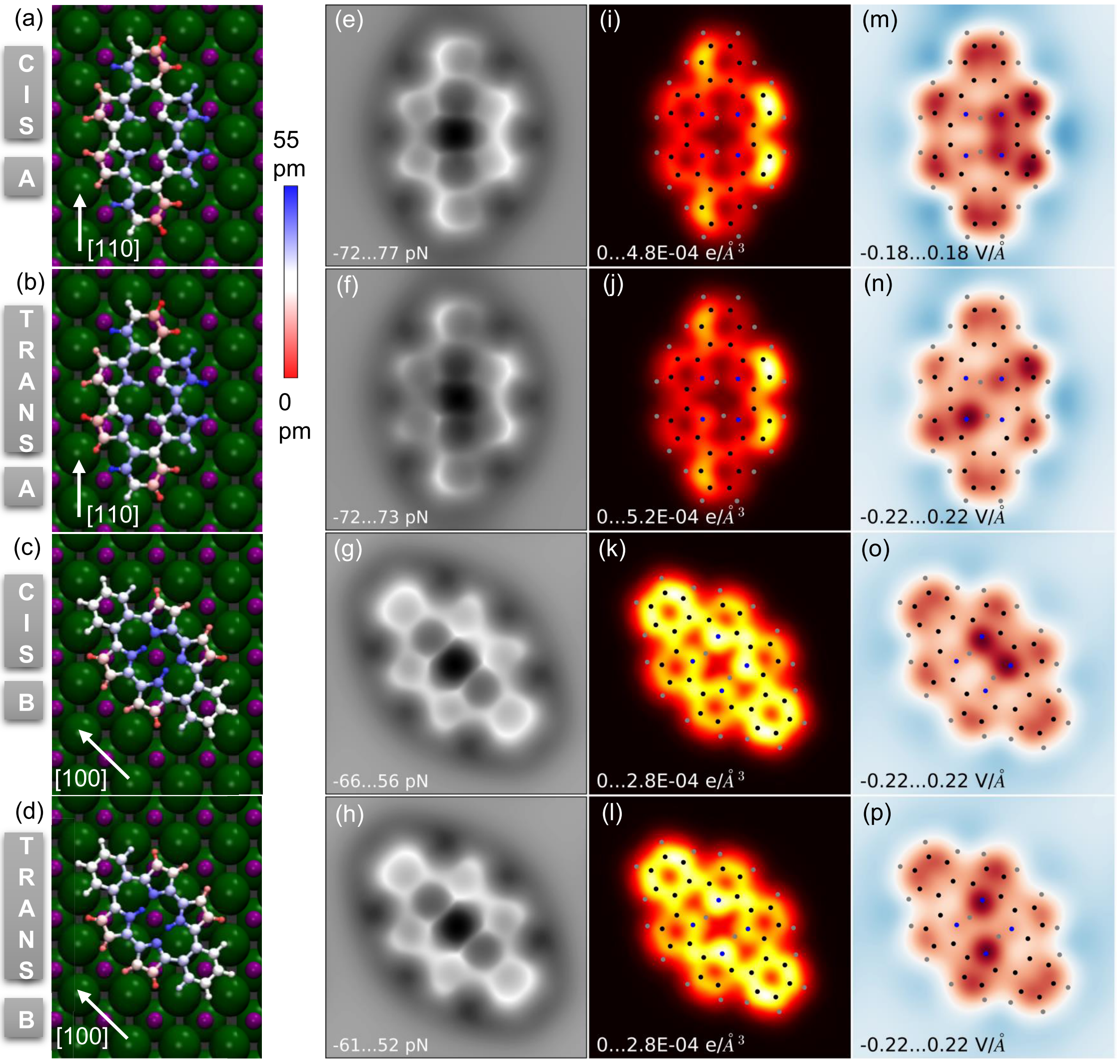

Figure 4. (a−d) Most stable structures for the cis (a, c) and trans (c, d) forms of the mDBPc molecule in configuration A (a, b) and configuration B (c, d) adsorbed on a NaCl surface, obtained from first-principles simulations. The color scale of the molecule represents the height of the atoms upon adsorption on the surface. 0 pm is set to the position of the atom closest to the substrate, and the white color in the color bar is associated with the surface−molecule distance at the mean plane (defined as the average of the z coordinates of all of the atoms in the molecule), The mean planes for (a), (b), (c), and (d) are 331, 331, 332, and 333 pm, respectively. The color code for the ball-and-stick model of the NaCl lattice is dark green for Cl and dark purple for Na. (e−h) Calculated constant-height force maps for the cis and trans-forms of the mDBPc molecule in configuration A (e, f) and configuration B (g, h), at a probe height of 3.1 Å from the average molecular plane. The black-to-white force scales are from −72 to 77 pN for (e), from −72 to 73 pN for (f), from −66 to 56 pN for (g), and from −61 to 52 pN for (h). (i−l) Calculated charge density maps, at 3 Å from the average molecular plane, for the cis and trans-forms of the mDBPc in configuration A (i, j) and configuration B (k, l), respectively. The highest charge density is expressed in yellow, and the lowest charge density is represented in black. (m−p) Simulated vertical component of the electric field, at 3 Å from the molecular plane, created by the cis and trans-forms of the mDBPc in configuration A (m, n) and configuration B (o, p), respectively. The highest positive value (electron attraction) is presented in blue and the lowest (electron repulsion) is displayed in red. In (i−p) the small dots represent the positions of atoms within the molecule: black for C, blue for N, and gray for H.

when the probe passes across certain points on the mDBPc molecule, so that always two pyrrole rings at the amine side are imaged. This flip is accompanied by a significant (∼0.2 nm) lateral displacement of the entire molecule along the short molecular axis. A careful observation of the AFM images (Figure 5c,d,g,h) and simultaneously obtained STM images (Figure 5e,f,i,j) enables finding the locations where the probe induces the flip. Images in Figure 5c,e,g,i are obtained by scanning from the left to the right, and those in Figure 5d,f,h,j are recorded from the right to the left. Instabilities under the probe appear as shaggy lines in these images, and their location depends on the scanning direction when the sample bias is set to negative values (Figure 5c−f). A high density of spikes and stripes in the AFM and STM signals appear close to the position where the two hydrogen atoms of the amine are located. When the sample bias is set to positive values (+500 mV in the case of Figure 5g−j) instabilities appear over the entire molecule. In the AFM images they are more visible at the edges of the molecule, and in the STM images, independent of the scan direction, a high density of instabilities is detected at the center of the molecule, extending over the long axis.

According to the theoretical calculations, H atom transfer within the Pc cavity of the mDBPc in configuration A should involve a lateral displacement of the entire molecule by 170 pm along the $[1\bar{1}0]$ direction. This agrees well with the value

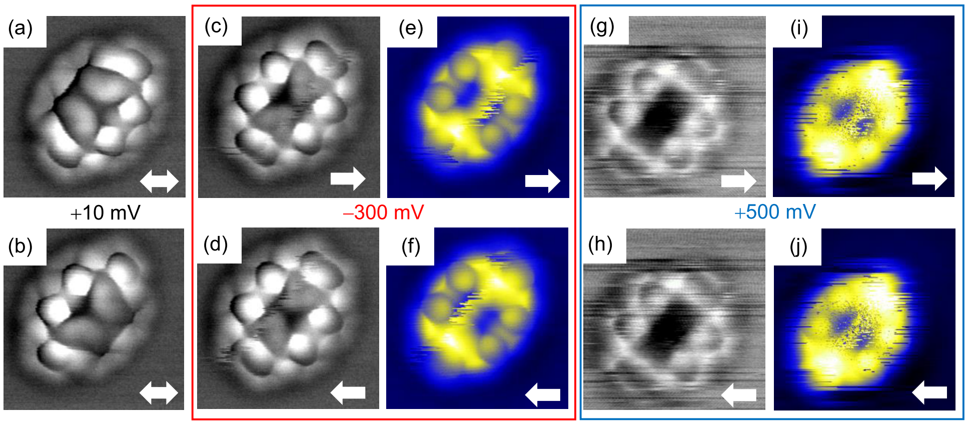

Figure 5. Hydrogen transfer within an mDBPc molecule in configuration A adsorbed on a bilayer thick NaCl island. (a and b) Constant-height Δf images of the same mDBPc molecule obtained with a sample bias of V_s = 10 mV, before (a) and after (b) inducing the H transfer within the molecule by a voltage pulse. At low bias voltages, no H-transfer during imaging acquisition is detected. (c and d) Constant-height Δf images of the same molecule but acquired at V_s = −300 mV. (e and f) Tunneling current (I_t) images simultaneously recorded with (c) and (d), respectively. (g and h) Constant-height Δf images of the same molecule but obtained with V_s = + 500 mV. (i and j) Tunneling current (I_t) images recorded simultaneously with (g) and (h), respectively. The scan directions of the images are indicated by white arrows. The scanned area is (2 nm × 2 nm). The Δf gray scale in (a−d) is from −0.6 (black) to 0.1 Hz (white). The I_t blue-yellow scale in (e, f) is from 0 (dark blue) to 4 pA (yellow-white). The Δf gray scale in (g, h) is from −0.86 (black) to −0.51 Hz (white). The I_t blue-yellow scale in (i, j) is from 1.5 (dark blue) to 11.5 pA (yellow-white).

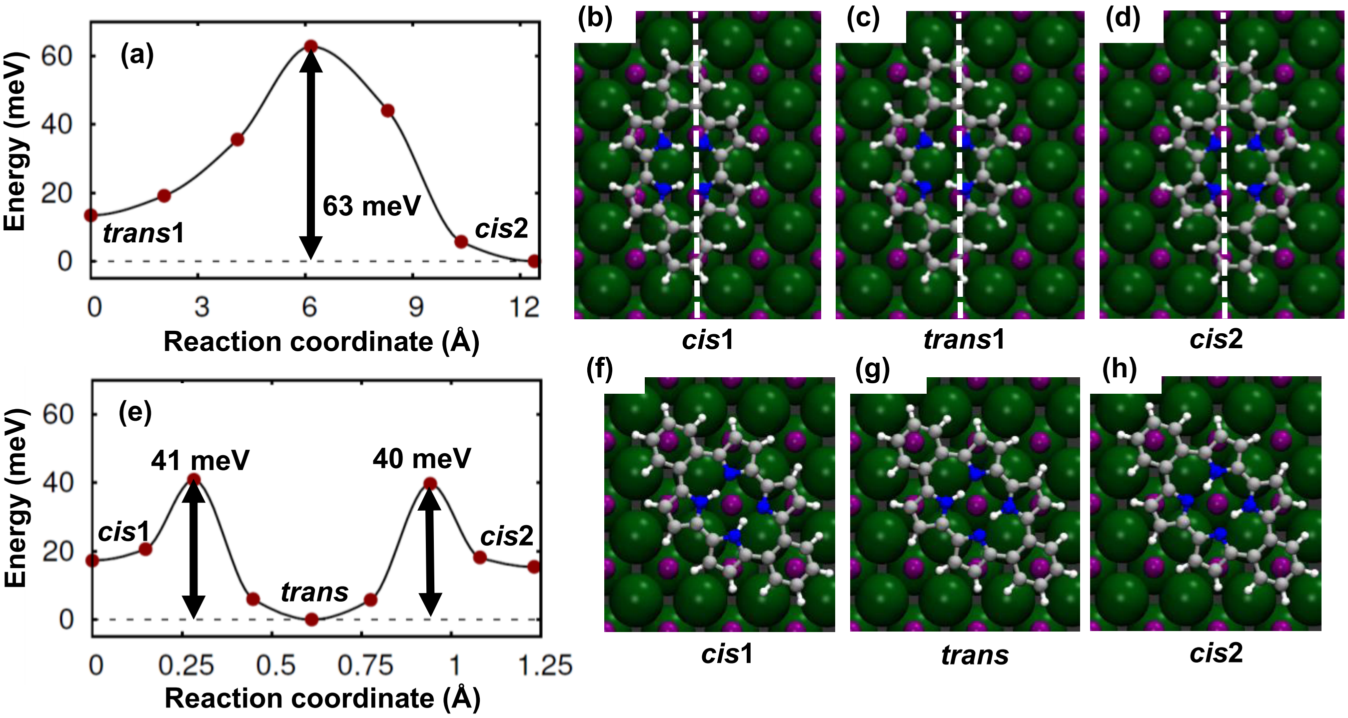

Figure 6. Calculated energy barriers for the tautomerization process, and adsorption configurations of the cis and trans-forms for the two adsorption geometries detected for an mDBPc molecule adsorbed on a NaCl bilayer. (a) Energy barrier between trans1 (c) and cis2 (d) for an mDBPc molecule in configuration A. (b−d) Adsorption geometries of cis1 (b), trans1 (c), and cis2 (d) for an mDBPc molecule in configuration A. Dotted white lines are drawn for an eye-guiding purpose to highlight the translation of the molecule during the process. (e) Energy barrier between trans and cis-forms of an mDBPc molecule in configuration B. (f−h) Adsorption configurations of cis1 (f), trans (g), and cis2 (g), for an mDBPc molecule in configuration B. The color code for the atomic species is dark green for Cl, dark purple for Na, gray for C, blue for N, and white for H.

experimentally found (∼0.2 nm), as well as with the fact that the mDBPc molecule appears widened when constant flips are induced by scanning as relatively high bias voltage values (Figure 5c,j). The calculated energy barrier for the H transfer with a lateral molecular displacement is 63 meV (Figure 6a). Note that this value is not significantly altered by the zero-point energy. We have performed dynamic calculations to account for the zero-point energy to correct the transition state energy by following the method provided in earlier reports[12,16,18] and confirmed that the barrier is lowered only by 7 meV. A small influence of the zero-point energy is mainly due to a weaker interaction of the mDBPc molecule with the NaCl substrate, compared to that with the metallic substrate. A previous theoretical study reported that the stronger the interaction of Pc with the metallic substrate, the higher the barrier energy correction by the zero-point energy becomes.[18]

The calculated adsorption configurations before and after the H transfer reaction, as shown in Figure 6b,d, confirm that the experimentally observed flips can be attributed to a tautomerization reaction with the lateral displacement of the entire molecule. Although two tautomeric forms on the same adsorption site, cis1 and trans1 (Figure 6b,c, respectively), are revealed in the process, they are indistinguishable in the experiments because of the similar appearance of their AFM and STM images. Here, we assume that the double H-transfer reaction occurs via a stepwise mechanism rather than in a concerted manner; that is, to achieve cis to cis tautomerization, the molecule should go through one of the trans configurations. Although both stepwise and concerted mechanisms compete in the gas phase,[39] the stepwise path was found to be more favorable for the Pc adsorbed on metallic surfaces.[15,16,18] Molecular dynamics simulations have also suggested that out-of-plane vibrational motions significantly decrease the contribution of the concerted proton transfer mechanism,[39] which may be relevant to the molecule considered in this study. Indeed, the calculated barrier for the concerted double H-transfer for the cis to cis tautomerization of mDBPc in configuration A on NaCl is 107 meV, which is much higher than the value for the stepwise mechanism from trans1 to cis2, 63 meV, as shown in Figure 6a. The barrier from cis1 to trans1 is even smaller, 40 meV.

The other adsorption orientation of the mDBPc molecule found on NaCl, the one with a symmetric appearance (configuration B), is oriented along the <100> direction. The calculated adsorption energies for its cis- and trans-forms only differ by 10 meV: the obtained values are 2.09 and 2.10 eV for cis and trans-forms, respectively. In contrast to configuration A, the tautomerization for configuration B does not involve any lateral displacement of the molecule, as shown in Figure 6f,h, and thus the energy barrier for the H-transfer within the Pc cavity is as low as ~40 meV (Figure 6e), which is close to the value in the gas phase. Because of the weak molecule−substrate interaction, the zero-point energy correction in configuration B is negligible, less than 0.5 meV.

■ CONCLUSIONS

We have investigated the adsorption behavior of mDBPc molecules on Ag(111) and on 2-ML-thick NaCl films using submolecular resolution AFM and STM. On the Ag(111) surface, the adsorption site and bonding nature are quite similar to those of the Pc molecule. The mDBPc exists in the cis tautomeric form with its two nonsaturated N atoms interacting with the Ag atoms of the substrate, giving rise to a height variation that causes an asymmetric appearance in the STM and AFM images. On NaCl, in contrast, two types of adsorption configurations are observed, which are due to a different orientation of the molecule with respect to the substrate lattice rather than to the tautomeric forms. Distinction between the cis and trans-forms was unattainable for both orientations on NaCl, but based on the comparison between experimental AFM images and simulated images, we found that the interaction with NaCl leads to very similar adsorption energies and a probe-molecule interaction force for both tautomers. The energy barrier between the cis and trans-forms on the same adsorption site is negligible, and thus the tautomerization reaction can be recognized only when it is accompanied by a lateral displacement of the molecule. Our results show the limitations of powerful imaging techniques like STM and AFM, where the symmetry of the molecules in the images is not, in general, directly correlated with the tautomeric forms. On the other hand, they prove that tautomerization reactions on rather inert ionic surfaces like NaCl are distinct from both those on metals and in the gas phase, revealing a new process that involves a global molecular translation upon H transfer. This novel tautomerization behavior might also be present on other weakly interacting substrates.

■ ASSOCIATED CONTENT

Supporting Information

The Supporting Information is available free of charge at https://pubs.acs.org/doi/10.1021/acs.jpcc.0c07726.

> Theoretical details; chemical structures, and ball-and-stick models of cis and trans-forms of mDBPc; submolecular resolution STM and AFM images of the same molecule before and after a flip; AFM images of mDBPc molecules on Ag(111) and on NaCl with superimposed lattice grids; frequency shift (Δf) -distance curves and slices of AFM images for the mDBPc molecule on Ag(111) and on NaCl; calculated force maps for the mDBPc molecule on Ag(111) and on NaCl at different probe-sample heights; and calculated component-force maps for the cis-form of mDBPc in configuration A on NaCl (PDF)

■ AUTHOR INFORMATION

Corresponding Authors

Ruben Perez − *Departamento de Física Teórica de la Materia Condensada and Condensed Matter Physics Center (IFIMAC), Universidad Autónoma de Madrid, E-28049 Madrid, Spain;* orcid.org/0000-0001-5896-541X; Email: ruben.perez@uam.es

Oscar Custance − *National Institute for Materials Science, Tsukuba, Ibaraki 305-0047, Japan;* Email: CUSTANCE.Oscar@nims.go.jp

Authors

Tomoko K. Shimizu − *Department of Applied Physics and Physico-Informatics, Faculty of Science and Technology, Keio University, Yokohama, Kanagawa 223-8522, Japan; National Institute for Materials Science, Tsukuba, Ibaraki 305-0047, Japan;* orcid.org/0000-0002-1301-0406

Carlos Romero-Muñiz − *Departamento de Física Teórica de la Materia Condensada, Universidad Autónoma de Madrid, E-28049 Madrid, Spain; Department of Physical, Chemical and Natural Systems, Universidad Pablo de Olavide, E-41013 Seville, Spain;* orcid.org/0000-0001-6902-1553

Oleksandr Stetsovych − *National Institute for Materials Science, Tsukuba, Ibaraki 305-0047, Japan; Institute of Physics, Academy of Sciences of the Czech Republic, 162 00 Prague 6, Czech Republic*

Jaime Carracedo-Cosme − *Departamento de Física Teórica de la Materia Condensada, Universidad Autónoma de Madrid, E-28049 Madrid, Spain; Quasar Science Resources S.L., E-28232 Las Rozas de Madrid, Spain*

Michael Ellner − *Departamento de Física Teórica de la Materia Condensada, Universidad Autónoma de Madrid, E-28049 Madrid, Spain*

Pablo Pou − *Departamento de Física Teórica de la Materia Condensada and Condensed Matter Physics Center (IFIMAC), Universidad Autónoma de Madrid, E-28049 Madrid, Spain*

Koji Oohora − *Department of Applied Chemistry, Graduate School of Engineering, Osaka University, Suita, Osaka 565-0871, Japan;* orcid.org/0000-0003-1155-6824

Takashi Hayashi − *Department of Applied Chemistry, Graduate School of Engineering, Osaka University, Suita, Osaka 565-0871, Japan;* orcid.org/0000-0002-2215-935X

Complete contact information is available at:
https://pubs.acs.org/10.1021/acs.jpcc.0c07726

Author Contributions

T.K.S., O.S., and O.C. performed experiments and data analysis. C.R.-M., J.C.-C., M.E., P.P. and R.P. carried out the first-principles calculations and analyzed the theoretical results. K.O. and T.H. synthesized the mDBPc molecule. T.K.S., C.R.M., P.P., R.P., and O.C. wrote the paper. All of the authors participated in the discussion of the results, read the paper, commented on the content, and agreed with the publication of the results.

Notes

The authors declare no competing financial interest.

■ ACKNOWLEDGMENTS

We thank Dr. Ayumu Ogawa for the help in synthesis of mDBPc. We are grateful for the financial support by the NIMS project (PF201) and by the MEXT KAKENHI Grant Numbers 26104540, 26104523, and 16H00837, and JSPS KAKENHI Grant Number 16K05674. O.S. thanks JSPS Postdoctoral Fellowship for Research in Japan. We thank the financial support from the Spanish MINECO (AEI/FEDER, UE, project MAT2017-83273-R), from MICINN through the “Maria de Maeztu“ Programme for Units of Excellence in R&D (CEX2018-000805-M), from Comunidad de Madrid Industrial Doctorate 2017 Program (reference IND2017/IND-7793), and from Quasar Science Resources S.L. The computer time provided by the Red Española de Supercomputación (RES) at the Marenostrum Supercomputer is also acknowledged.

■ REFERENCES

(1) Auwärter, W.; Seufert, K.; Bischoff, F.; Ecija, D.; Vijayaraghavan, S.; Joshi, S.; Klappenberger, F.; Samudrala, N.; Barth, J. V. A Surface-Anchored Molecular Four-Level Conductance Switch Based on Single Proton Transfer. *Nat. Nanotechnol.* **2012**, *7*, 41−46.

(2) Liljeroth, P.; Repp, J.; Meyer, G. Current-Induced Hydrogen Tautomerization and Conductance Switching of Naphthalocyanine Molecules. *Science* **2007**, *317*, 1203−1206.

(3) Liu, J.; Li, C.; Liu, X.; Lu, Y.; Xiang, F.; Qiao, X.; Cai, Y.; Wang, Z.; Liu, S.; Wang, L. Positioning and Switching Phthalocyanine Molecules on a Cu(100) Surface at Room Temperature. *ACS Nano* **2014**, *8*, 12734−12740.

(4) Kügel, J.; Klein, L.; Leisegang, M.; Bode, M. Analyzing and Tuning the Energetic Landscape of H_2Pc Tautomerization. *J. Phys. Chem. C* **2017**, *121*, 28204−28210.

(5) Doppagne, B.; Neuman, T.; Soria-Martinez, R.; López, L. E. P.; Bulou, H.; Romeo, M.; Berciaud, S.; Scheurer, F.; Aizpurua, J.; Schull, G. Single-Molecule Tautomerization Tracking through Space- and Time-Resolved Fluorescence Spectroscopy. *Nat. Nanotechnol.* **2020**, *15*, 207−211.

(6) Kozlowski, P. M.; Jarzęcki, A. A.; Pulay, P. Vibrational Assignment and Definite Harmonic Force Field for Porphine. 1. Scaled Quantum Mechanical Results and Comparison with Empirical Force Field. *J. Phys. Chem. A.* **1996**, *100*, 7007−7013.

(7) Waluk, J. Ground- and Excited-State Tautomerism in Porphycenes. *Acc. Chem. Res.* **2006**, *39*, 945−952.

(8) Kumagai, T.; Hanke, F.; Gawinkowski, S.; Sharp, J.; Kotsis, K.; Waluk, J.; Persson, M.; Grill, L. Thermally and Vibrationally Induced Tautomerization of Single Porphycene Molecules on a Cu(110) Surface. *Phys. Rev. Lett.* **2013**, *111*, No. 246101.

(9) Kumagai, T.; Hanke, F.; Gawinkowski, S.; Sharp, J.; Kotsis, K.; Waluk, J.; Persson, M.; Grill, L. Controlling Intramolecular Hydrogen Transfer in a Porphycene Molecule with Single Atoms or Molecules Located Nearby. *Nat. Chem.* **2014**, *6*, 41−46.

(10) Ladenthin, J. N.; Grill, L.; Gawinkowski, S.; Liu, S.; Waluk, J.; Kumagai, T. Hot Carrier-Induced Tautomerization within a Single Porphycene Molecule on Cu(111). *ACS Nano* **2015**, *9*, 7287−7295.

(11) Böckmann, H.; Liu, S.; Mielke, J.; Gawinkowski, S.; Waluk, J.; Grill, L.; Wolf, M.; Kumagai, T. Direct Observation of Photoinduced Tautomerization in Single Molecules at a Metal Surface. *Nano Lett.* **2016**, *16*, 1034−1041.

(12) Ladenthin, J. N.; Frederiksen, T.; Persson, M.; Sharp, J. C.; Gawinkowski, S.; Waluk, J.; Kumagai, T. Force-Induced Tautomerization in a Single Molecule. *Nat. Chem.* **2016**, *8*, 935−940.

(13) Böckmann, H.; Müller, M.; Hammud, A.; Willinger, M. G.; Pszona, M.; Waluk, J.; Wolf, M.; Kumagai, T. Near-Field Spectral Response of Optically Excited Scanning Tunneling Microscope Junctions Probed by Single-Molecule Action Spectroscopy. *J. Phys. Chem. Lett.* **2019**, *10*, 2068−2074.

(14) Böckmann, H.; Gawinkowski, S.; Waluk, J.; Raschke, M. B.; Wolf, M.; Kumagai, T. Near-Field Enhanced Photochemistry of Single Molecules in a Scanning Tunneling Microscope Junction. *Nano Lett.* **2018**, *18*, 152−157.

(15) Kumagai, T.; Ladenthin, J. N.; Litman, Y.; Rossi, M.; Grill, L.; Gawinkowski, S.; Waluk, J.; Persson, M. Quantum Tunneling in Real Space: Tautomerization of Single Porphycene Molecules on the (111) Surface of Cu, Ag, and Au. *J. Chem. Phys.* **2018**, *148*, No. 102330.

(16) Koch, M.; Pagan, M.; Persson, M.; Gawinkowski, S.; Waluk, J.; Kumagai, T. Direct Observation of Double Hydrogen Transfer via Quantum Tunneling in a Single Porphycene Molecule on a Ag(110) Surface. *J. Am. Chem. Soc.* **2017**, *139*, 12681−12687.

(17) Kumagai, T. Direct Observation and Control of Hydrogen-Bond Dynamics Using Low-Temperature Scanning Tunneling Microscopy. *Prog. Surf. Sci.* **2015**, *90*, 239−291.

(18) Li, J.; Yang, S.; Ren, J. C.; Su, G.; Li, S.; Butch, C. J.; Ding, Z.; Liu, W. Deep Molecular Orbital Driven High-Temperature Hydrogen Tautomerization Switching. *J. Phys. Chem. Lett.* **2019**, *10*, 6755−6761.

(19) Sarma, T.; Panda, P. K. Annulated Isomeric, Expanded, and Contracted Porphyrins. *Chem. Rev.* **2017**, *117*, 2785−2838.

(20) Waluk, J. Spectroscopy and Tautomerization Studies of Porphycenes. *Chem. Rev.* **2017**, *117*, 2447−2480.

(21) Oohora, K.; Ogawa, A.; Fukuda, T.; Onoda, A.; Hasegawa, J. Y.; Hayashi, T. Meso-Dibenzoporphycene Has a Large Bathochromic Shift and a Porphycene Framework with an Unusual Cis Tautomeric Form. *Angew. Chem., Int. Ed.* **2015**, *54*, 6227−6230.

(22) Kozlowski, P. M.; Zgierski, M. Z.; Baker, J. The Inner-Hydrogen Migration and Ground-State Structure of Porphycene. *J. Chem. Phys.* **1998**, *109*, 5905−5913.

(23) Mohn, F.; Gross, L.; Moll, N.; Meyer, G. Imaging the Charge Distribution within a Single Molecule. *Nat. Nanotechnol.* **2012**, *7*, 227−231.

(24) Albrecht, T. R.; Grütter, P.; Horne, D.; Rugar, D. Frequency Modulation Detection Using High-Q Cantilevers for Enhanced Force Microscope Sensitivity. *J. Appl. Phys.* **1991**, *69*, 668−673.

(25) Bartels, L.; Mayer, G.; Rieder, K.-H.; Velic, D.; Knoesel, E.; Hotzel, A.; Wolf, M.; Ertl, G. Dynamics of Electron-Induced Manipulation of Individual CO Molecules on Cu(111). *Phys. Rev. Lett.* **1998**, *80*, 2004−2007.

(26) Gross, L.; Mohn, F.; Moll, N.; Liljeroth, P.; Meyer, G. The Chemical Structure of a Molecule Resolved by Atomic Force Microscopy. *Science* **2009**, *325*, 1110−1114.

(27) Heinrich, A. J.; Lutz, C. P.; Gupta, J. A.; Eigler, D. M. Molecule Cascades. *Science* **2002**, *298*, 1381−1387.

(28) Kresse, G.; Furthmüller, J. Efficient Iterative Schemes for Ab Initio Total-Energy Calculations Using a Plane-Wave Basis Set. *Phys. Rev. B* **1996**, *54*, 11169−11186.

(29) Blöchl, P. E. Projector Augmented-Wave Method. *Phys. Rev. B* **1994**, *50*, 17953−17979.

(30) Perdew, J. P.; Burke, K.; Ernzerhof, M. Generalized Gradient Approximation Made Simple. *Phys. Rev. Lett.* **1996**, *77*, 3865−3868.

(31) Grimme, S.; Antony, J.; Ehrlich, S.; Krieg, H. A Consistent and Accurate Ab Initio Parametrization of Density Functional Dispersion Correction (DFT-D) for the 94 Elements H-Pu. *J. Chem. Phys.* **2010**, *132*, No. 154104.

(32) Henkelman, G.; Uberuaga, B. P.; Jónsson, H. Climbing Image Nudged Elastic Band Method for Finding Saddle Points and Minimum Energy Paths. *J. Chem. Phys.* **2000**, *113*, 9901−9904.

(33) Ellner, M.; Pou, P.; Pérez, R. Molecular Identification, Bond Order Discrimination, and Apparent Intermolecular Features in Atomic Force Microscopy Studied with a Charge Density Based Method. *ACS Nano* **2019**, *13*, 786−795.

(34) Ellner, M.; Pou, P.; Pérez, R. Atomic Force Microscopy Contrast with CO Functionalized Tips in Hydrogen-Bonded Molecular Layers: Does the Real Tip Charge Distribution Play a Role? *Phys. Rev. B* **2017**, *96*, No. 075418.

(35) Ellner, M.; Pavliček, N.; Pou, P.; Schuler, B.; Moll, N.; Meyer, G.; Gross, L.; Peréz, R. The Electric Field of CO Tips and Its Relevance for Atomic Force Microscopy. *Nano Lett.* **2016**, *16*, 1974−1980.

(36) Kresse, G.; Joubert, D. From Ultrasoft Pseudopotentials to the Projector Augmented-Wave Method. *Phys. Rev. B* **1999**, *59*, 1758−1775.

(37) van der Lit, J.; Di Cicco, F.; Hapala, P.; Jelinek, P.; Swart, I. Submolecular Resolution Imaging of Molecules by Atomic Force Microscopy: The Influence of the Electrostatic Force. *Phys. Rev. Lett.* **2016**, *116*, No. 096102.

(38) Hapala, P.; Temirov, R.; Tautz, F. S.; Jelínek, P. Origin of High-Resolution IETS-STM Images of Organic Molecules with Functionalized Tips. *Phys. Rev. Lett.* **2014**, *113*, No. 226101.

(39) Yoshikawa, T.; Sugawara, S.; Takayanagi, T.; Shiga, M.; Tachikawa, M. Quantum Tautomerization in Porphycene and Its Isotopomers: Path-Integral Molecular Dynamics Simulations. *Chem. Phys.* **2012**, *394*, 46−51.